

On the domain size for the steady-state CFD modelling of a tall building

J. Revuz¹, D.M. Hargreaves*² and J.S. Owen²

¹Anslys France, Montigny le Bretonneux, France

²Faculty of Engineering, The University of Nottingham, Nottingham, UK

(Received June 27, 2011, Revised July 14, 2011, Accepted August 23, 2011)

Abstract. There have existed for a number of years good practice guidelines for the use of Computational Fluid Dynamics (*CFD*) in the field of wind engineering. As part of those guidelines, details are given for the size of flow domain that should be used around a building of height, H . For low-rise buildings, the domain sizes produced by following the guidelines are reasonable and produce results that are largely free from blockage effects. However, when high-rise or tall buildings are considered, the domain size based solely on the building height produces very large domains. A large domain, in most cases, leads to a large cell count, with many of the cells in the grid being used up in regions far from the building/wake region. This paper challenges this domain size guidance by looking at the effects of changing the domain size around a tall building. The *RNG* k - ε turbulence model is used in a series of steady-state solutions where the only parameter varied is the domain size, with the mesh resolution in the building/wake region left unchanged. Comparisons between the velocity fields in the near-field of the building and pressure coefficients on the building are used to inform the assessment. The findings of the work for this case suggest that a domain of approximately 10% the volume of that suggested by the existing guidelines could be used with a loss in accuracy of less than 10%.

Keywords: tall buildings; CFD; domain

1. Introduction

The authors have recently been working on the Computational Fluid Dynamics (*CFD*) modelling of flexible tall buildings in turbulent inflows (Revuz *et al.* 2010). A key part of the modelling is the choice of the domain size and the positioning of the single tall building within that domain. Recent CFD studies have used Franke *et al.* (2004) as a starting point in determining the domain size. The relevant section from Franke *et al.* (2004) is as follows

“The inlet, the lateral and the top boundary should be $5H$ away from the building, where H is the building height. For buildings with an extension in the lateral direction much larger than the height, the blockage ratio should be below 3% [38]. The outflow boundary should be positioned at least $15H$ behind the building to allow for flow development...this outflow length should also be applied for an urban area with many buildings, where H is replaced by H_{max} , the height of the tallest building. To prevent artificial acceleration of the flow over the tallest building, the top of the

* Corresponding author, Lecturer, E-mail: david.hargreaves@nottingham.ac.uk

computational domain should be also at least $5 H_{\max}$ away from this building.”

In the quote, reference [38] refers to Baetke and Werner (1990). A later document (Franke *et al.* 2007) updates these recommendations and, in particular, states

“...a single building of height H with quadratic projected area in the flow direction”

which the authors here interpret as referring to a low-rise building. Franke *et al.* (2007) go on to say

“For buildings with an extension in the lateral direction much larger than the height, the blockage should also be below the maximum allowed value. In that case the ratio of the lateral extension of the computational domain to its height should be similar to the corresponding ratio for the building (Blocken *et al.* 2004).”

If the same argument were used for buildings where $H \gg B$, then the width of the domain, assuming a conservative blockage ratio of 1.5%, would be $13B$. As will be shown in this paper, this width is far too small to maintain accuracy and again shows that the recommendations of Franke *et al.* (2007) require some modifications for large frontal aspect ratio buildings. The report also refers to a Verein Deutscher Ingenieure (VDI 2000) publication which suggests that the blockage ratio should be less than 10%, based largely on wind tunnel modelling experience, which is above the 3% recommended by Franke *et al.* (2004).

There is considerable evidence of these recommendations being adhered to by workers when modelling low-rise buildings. For example, Fig. 1 is taken from Franke (2007) and shows the domain used to model the Silsoe cube (Hoxey *et al.* 2002). For such low-rise buildings, where $H \sim B \sim L$ (with B and L being the cross- and alongwind building dimensions respectively), these requirements produce domains that are both acceptable in physical and computational terms. By “acceptable in...computational terms”, it is meant that the domain boundaries are not so distant from the building that the number of computational cells required to fill the domain to ensure a reasonable level of accuracy becomes too large.

However, when the aspect ratio of the building changes and $H \gg L, B$, as is the case for tall buildings, the domain size chosen by workers is open to more interpretation. There is a small, but increasing, body of work using *CFD* to model wind loads on, pedestrian level comfort close to, and rainfall around tall buildings. By analysing this work, it has been possible to assemble Table 1, which includes the guidelines for comparison. Wherever possible in this table, the length of the domain, l , is shown as a sum of three components: l_u , L and l_d , the upstream fetch, the building length in the alongwind direction and the downwind fetch respectively. Similarly, the width of the

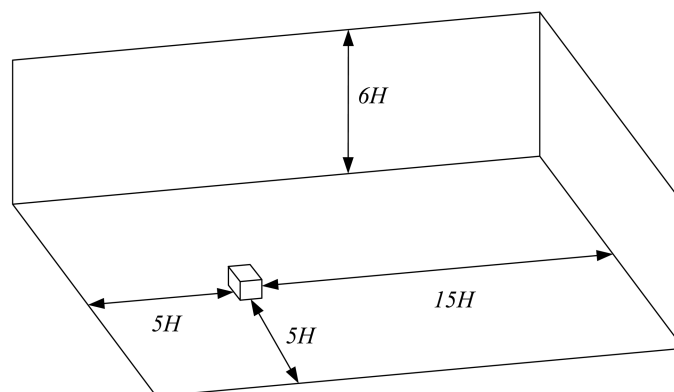


Fig. 1 A reproduction of the domain used by Franke (2007) when modelling the Silsoe Cube

Table 1 Domain sizes from relevant CFD modelling of tall buildings

	Domain			Building
	l	b	h	H (m)
Sankaran and Paterson (1997) ^a	?	?	?	183
Watakabe <i>et al.</i> (2002) ^b	$28H$	$18H$	$25H$	31.2
Mochida <i>et al.</i> (2002) ^c	$10.8H$	$6.9H$	$5.6H$	0.16
Franke <i>et al.</i> (2004)	$5H + L + 15H$	$5H + B + 5H$	$H + 5H$	
So <i>et al.</i> (2005) ^d	$20H$	$10H$	$20H$?
Huang <i>et al.</i> (2007)	$1.5H + L + 5.5H$	$2H + B + 2H$	$2H$	183
Tominaga <i>et al.</i> (2008) ^e	$? + L + 10H$	$5H + B + 5H$	$H + 5H$?
Braun and Awruch (2009)	$3H + L + 8H$	$2.2H + B + 2.2H$	$H + 3.5H$	180

^aThe building occupied the central $12 \times 12 \times 12$ cells of a $46 \times 42 \times 46$ grid.

^bThese are general guidelines, but the implication in the paper is that they are applicable for tall buildings.

^cThe domain size was constrained to be the same size as the wind tunnel used in the experiments of Ishihaba and Hibi (1998). Here the aspect ratio, H/B , was 2.

^dA street canyon with tall buildings was modelled here, so it is of only passing relevance.

^e H in this case is defined as the height between the fifth and sixth levels in the building, but the figures in the paper do not support this.

domain, b , is broken into three components: b_a , B and b_g (most domains are symmetrical and so $b_d = b_g$, typically). The height of the domain, h , has only two components: H and h_s , the latter being the distance from the top of the building to the top of the domain. Due to the scarcity of reported work, cases with a single building, two buildings and arrays of buildings, one of which might be tall, are considered in the table. The overall impression from the literature is that very few tall buildings have been modelled using *CFD* by the academic community and what there is does not resemble the Franke *et al.* (2004) guidelines, except perhaps for Tominaga *et al.* (2008). Clearly, some of the work presented in Table 1 predates the guidelines, but the impression remains.

This paper sets out to determine the sensitivity of pressure coefficients and velocity fields to the size of domain around a tall building. A similar study was carried out by Xiang and Wang (2008), but for low-rise buildings with a fixed domain height. Buccolieri and Di Sabatino (2007) looked at the influence of domain size on an array of buildings, effectively challenging the best practice guidelines of Franke *et al.* (2004) for the case of pollution dispersion in an array of buildings.

It is important to note that it is not the object of this work to study different mesh resolutions, turbulence models, boundary conditions, etc., but is simply to extend a small domain incrementally to test the effect of moving the boundaries. However, details of a sensitivity study on this and other tall buildings to mesh and turbulence models can be found in Revuz (2011). Indeed, the use of a steady Reynolds-Average Navier-Stokes turbulence model, such as used in the present work, in the context of predicting wind loads on buildings is widely accepted as having problems (Tamura *et al.* 2008). The test case described in Section 2 is for a 1:200 scale 180 m building, with a large aspect ratio. A 1:200 scale building was used because in other parts of the work of Revuz (2011), Large Eddy Simulations (*LES*) were used, so that using a scale model resulted in smaller Reynolds number flows. The present work was motivated by the fact that the recommendations of Franke *et al.* (2004) for the size of the domain lead to very large domains for high rise buildings. This is

largely due to H being used as the characteristic length scale upon which the dimensions of the domain are based. The resulting large domain implies a very large number of cells, which is expensive in terms of computing power and time. The underlying idea was therefore to inform new, practical recommendations for the size of the domain for tall buildings.

2. Case study

The computational work described in this paper was carried out using ANSYS Fluent, version 12.1.4.

2.1 Domains and meshes

The building chosen for this work is a 1:200 scale rectangular prism with full-scale dimensions of $H = 180$ m, $L = 10$ m and $B = 20$ m (0.9 m by 0.05 m by 0.1 m at scale). This prism is placed in a rectangular domain, the dimensions of which are varied. Four domains were initially created for the study, with a further domain (Proposed) added later, and all are shown schematically in Fig. 2,

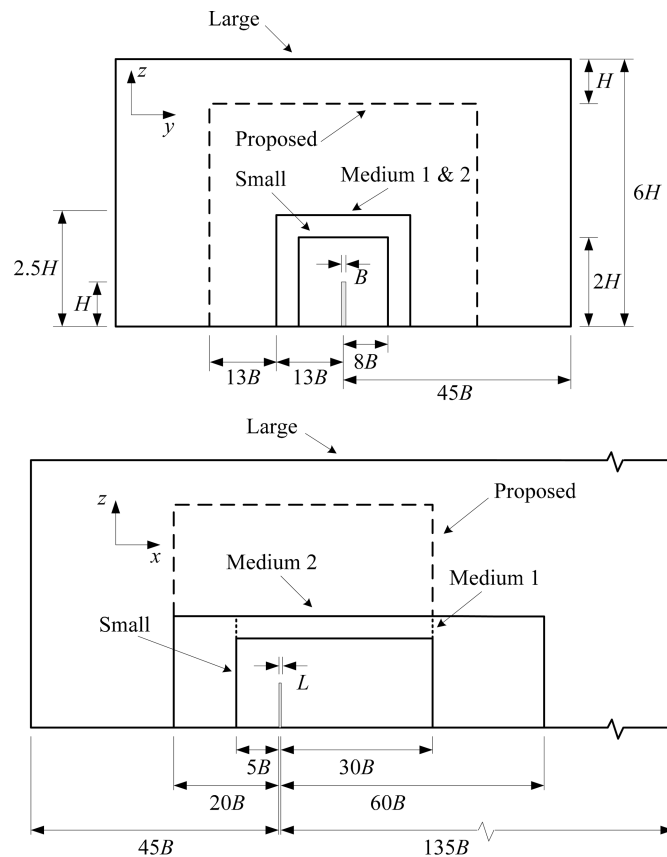


Fig. 2 Dimension of all the domains used in the study

Table 2 Characteristics of the domains used in the study. B.R. stands for blockage ratio. The drag coefficient, C_d , is also included

	Small	Medium 1	Medium 2	Large	Proposed
Length, l	$5B + L + 30B$	$5B + L + 30B$	$20B + L + 60B$	$45B + L + 135B$	$20B + L + 30B$
Width, b	$8B + B + 8B$	$13B + B + 13B$	$13B + B + 13B$	$45B + B + 45B$	$26B + B + 26B$
Height, h	$H + H$	$H + 1.5H$	$H + 1.5H$	$H + 5H$	$H + 4H$
B.R.yz-plane	3%	1.5%	1.5%	0.18%	0.36%
B.R.y-dir.	6%	3.7%	3.7%	0.8%	2%
B.R.z-dir.	50%	40%	40%	16%	20%
Cell count	1.2×10^6	1.5×10^6	2.1×10^6	5.0×10^6	3.5×10^6
C_d	1.205	1.205	1.147	1.058	1.088

which shows the coordinate system used, specifically the alignment of the zx - and yz -planes. The dimensions, blockage ratios and the number of cells used in each domain are listed in Table 2 and the domains are briefly summarised thus

Small with a 3% blockage ratio (ratio of the front area of the building over the inlet area) and upstream and downstream fetches based on the building width, B .

Medium 1 which is an extension of the small domain, but only in the yz -plane, to create a 1.5% blockage ratio.

Medium 2 which has the same blockage ratio as the Medium 1 domain, but is extended upwind and downstream.

Large which was built according to the recommendations of Franke *et al.* (2007).

Proposed which was based on the findings of the present study and represents the recommended domain size for studies of this nature.

Since the aim of this work was to study the influence of the size of the domain on the flow field around the building and in the wake, the mesh adjacent to the building and in its wake remained the same throughout, so any differences in the wind flow will be due to a change in the size of the domain and not the mesh adjacent to the building. In fact, the small domain was extended by adding blocks around it, of increasing cell size, to create the required domain sizes. All the meshes consisted entirely of hexahedral cells. The normal cell size next to the building was 5×10^{-4} m and the maximum cell size for the Small, Medium 1 and Medium 2 meshes was 0.06 m, while for the Large domain, well away from the building, it was 0.18 m.

Fig. 3(a) shows a close up of the surface mesh close to the foot of the building and highlights the growth of the cells in the boundary layer next to the building. Clearly the aspect ratios of these boundary layer cells are very large, but as Spalart (2001) indicates, there is no formal restriction on the size of cells in the wall-parallel direction in RANS simulations. However, Spalart (2001) is discussing streamlined bodies, not the complex detached flows seen with the bluff body under discussion here. A second view of the mesh is shown in Fig. 3(b), which shows that the mesh was more refined in the wake region relative to the more distant regions of the domain.

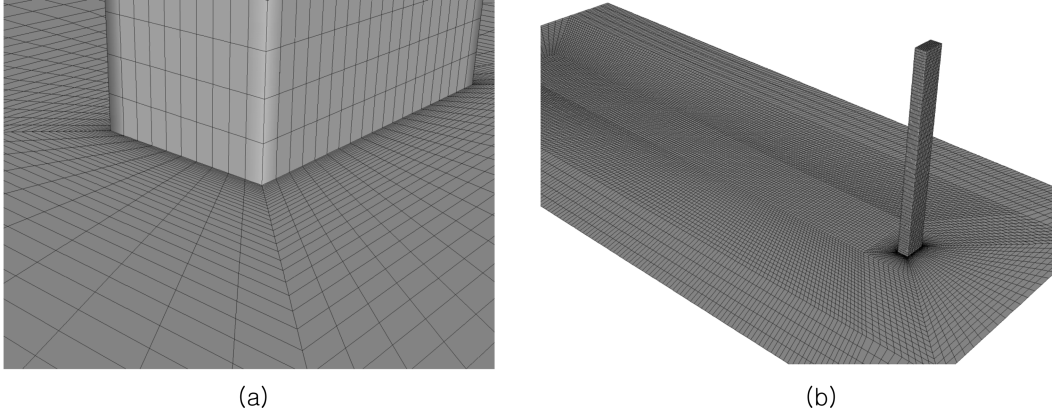


Fig. 3 Surface meshes for the small domain showing (a) the region around the base of the building and (b) the building and wake region

2.2 Governing equations

For completeness, there follows a description of the governing equations solved, including those for the turbulence model used - the *RNG k-ε*. If the various flow properties such as velocity, for example, are considered to consist of a mean or time-averaged part, U_i , and a time-varying part, u'_i , the instantaneous velocity, u_i , could be written as

$$u_i = U_i + u'_i \quad (1)$$

The Reynolds-Averaged Navier-Stokes (*RANS*) equations can be written in tensor notation as, first, the continuity equation

$$\frac{\partial}{\partial x_i}(\rho U_i) = 0 \quad (2)$$

where ρ is the density of the fluid and second, the conservation of momentum equation

$$\frac{\partial}{\partial x_j}(\rho U_i U_j) = -\frac{\partial P}{\partial x_i} + \frac{\partial}{\partial x_j} \left[\mu \left(\frac{\partial U_i}{\partial x_j} + \frac{\partial U_j}{\partial x_i} \right) \right] + \frac{\partial}{\partial x_j} (-\rho \overline{u'_i u'_j}) \quad (3)$$

where P is the mean pressure and μ is the dynamic viscosity. The terms

$$-\rho \overline{u'_i u'_j} \quad (4)$$

are referred to as the Reynolds Stresses, τ_{ij} , and represent six (due to symmetry) additional unknowns into the *RANS* equations that must be modelled in some way to allow for the solution of Eqs. (2) and (3). The Boussinesq Approximation can be used in which the Reynolds Stresses are related to the mean rates of deformation of the fluid

$$-\rho \overline{u'_i u'_j} = \mu_t \left(\frac{\partial U_i}{\partial x_j} + \frac{\partial U_j}{\partial x_i} \right) - \frac{2}{3} k \delta_{ij} \quad (5)$$

where μ_t is the turbulent (or eddy) viscosity, k is the turbulent kinetic energy and δ_{ij} is the Kroeneker delta function. A large number of turbulence models have been developed over the years based on this eddy viscosity approach and one class, the so-called two-equation models, have achieved temporary pre-eminence in engineering applications, due to their wide-range of applicability and relatively low computational costs.

Such a two-equation model is the standard k - ε (Launder and Spalding 1974). The transport equation for k is mathematically derived whilst the dissipation rate, ε , is based upon empirical definitions. In the two-equation approach, the eddy viscosity is formulated as

$$\mu_t = \rho C_\mu \frac{k^2}{\varepsilon} \quad (6)$$

where C_μ is a constant in Launder and Spalding's (1974) model. However, the standard k - ε model is known to perform poorly for the types of flows seen in wind engineering that involve separation and steep pressure gradients. In the present work, the *RNG* k - ε model (Yakhot *et al.* 1992) was used

$$\frac{\partial}{\partial x_j}(\rho k U_j) = \frac{\partial}{\partial x_j} \left[\left(\mu + \frac{\mu_t}{\sigma_k} \right) \frac{\partial k}{\partial x_j} \right] + P_k - \rho \varepsilon \quad (7)$$

$$\frac{\partial}{\partial x_j}(\rho \varepsilon U_j) = \frac{\partial}{\partial x_j} \left[\left(\mu + \frac{\mu_t}{\sigma_\varepsilon} \right) \frac{\partial \varepsilon}{\partial x_j} \right] + C_{1s} \frac{\varepsilon}{k} P_k - C_{2s}^* \rho \frac{\varepsilon^2}{k} \quad (8)$$

where the effects of compressibility and buoyancy on turbulence have been neglected. The term, $P_k = m_t S^2$, represents the production rate of turbulent kinetic energy, with $S = (2S_{ij}S_{ij})^{1/2}$ being the modulus of the mean rate of strain tensor. The key difference between the standard and *RNG* k - ε models is the coefficient, C_{2s}^* , which is given by

$$C_{2s}^* = C_{2s} + \frac{C_\mu \eta^3 \left(1 - \frac{\eta}{\eta_0} \right)}{1 + \beta \eta^3} \quad (9)$$

where $\eta = Sk/\varepsilon$. The model constants, C_μ , σ_k , σ_ε , C_{1s} , C_{2s} and η_0 are derived explicitly and have values of 0.0845, 0.719, 0.719, 1.42, 1.68 and 4.38 respectively. Only β , whose value is 0.012, has been derived from experiment. The *RNG* k - ε model has been shown by Kim and Baik (2004) to be accurate in predicting pollution dispersion in the urban environment. In addition, Etyemezian *et al.* (2000) used the *RNG* k - ε model when assessing the rainfall distribution on a tall building, with some success.

2.3 Boundary and initial conditions

At the upwind boundary, a velocity inlet was used and the following expressions for the alongwind component of velocity, U , the turbulent kinetic energy, k and its dissipation rate, ε from Richards and Hoxey (1993) were used

$$U(z) = \frac{u_*}{\kappa} \ln\left(\frac{z+z_0}{z_0}\right) \quad (10)$$

$$k(z) = \frac{u_*^2}{\sqrt{C_\mu}} \quad (11)$$

$$\varepsilon(z) = \frac{u_*^3}{\kappa(z+z_0)} \quad (12)$$

where κ is von Karman's constant and z_0 is the surface roughness length. Eq. (10) is a standard representation of the velocity profile in the *ABL*. In the present work, $z_0 = 0.001$ m and $u_* = 0.11$ ms⁻¹. The standard coefficients of the *RNG* k - ε model were used. The Reynolds number for the flow is 1.2×10^5 , using the building height, H , and the velocity at $z = H$ as reference values.

At the downwind boundary, a pressure outlet was used, with the relative pressure specified at 0 Pa and backflow conditions for k and ε set to those of the inlet. In all domains, however, backflow was not observed because the downwind boundary was sufficiently far from the building. The low- and high- y boundaries were set as symmetry conditions, as was the high- z boundary. A shear stress was applied at the top boundary via a momentum source term in the layer of cells adjacent to the symmetry boundary, as suggested by Richards and Hoxey (1993). On the low- z boundary, a rough wall was specified to model the effect of the ground roughness. According to Blocken *et al.* (2007), the constant, k_s , in the law of the wall was specified as

$$k_s = \frac{9.793}{C_s} z_0 = 1.96 \times 10^{-2} \text{ m} \quad (13)$$

with C_s taking its default value of 0.5. The walls of the building were specified as smooth. Eqs. (10) to (12) were used to specify the field variables throughout the domain as initial conditions at the start of the steady-state simulation.

2.4 Solver settings

As mentioned in Section 2.3, the solutions were steady-state. Second-order differencing was used for the pressure, momentum and turbulence equations and the "coupled" pressure-velocity coupling approach due to its robustness for steady-state, single-phase flow problems. The residuals fell below the commonly applied criteria of falling to 10^{-4} of their initial values after several hundred iterations. However, this was not the only test for convergence - the drag, lift and side forces and the moments acting on the building were monitored during the simulation and only when they achieved stationary values were the simulations deemed to have converged. Although the simulations were steady-state, there was some variation (< 1%) in the "steady" values of the various monitoring values.

3. Results and discussion

Fig. 4 shows contour plots of the velocity magnitude at the mid-height of the building for the four

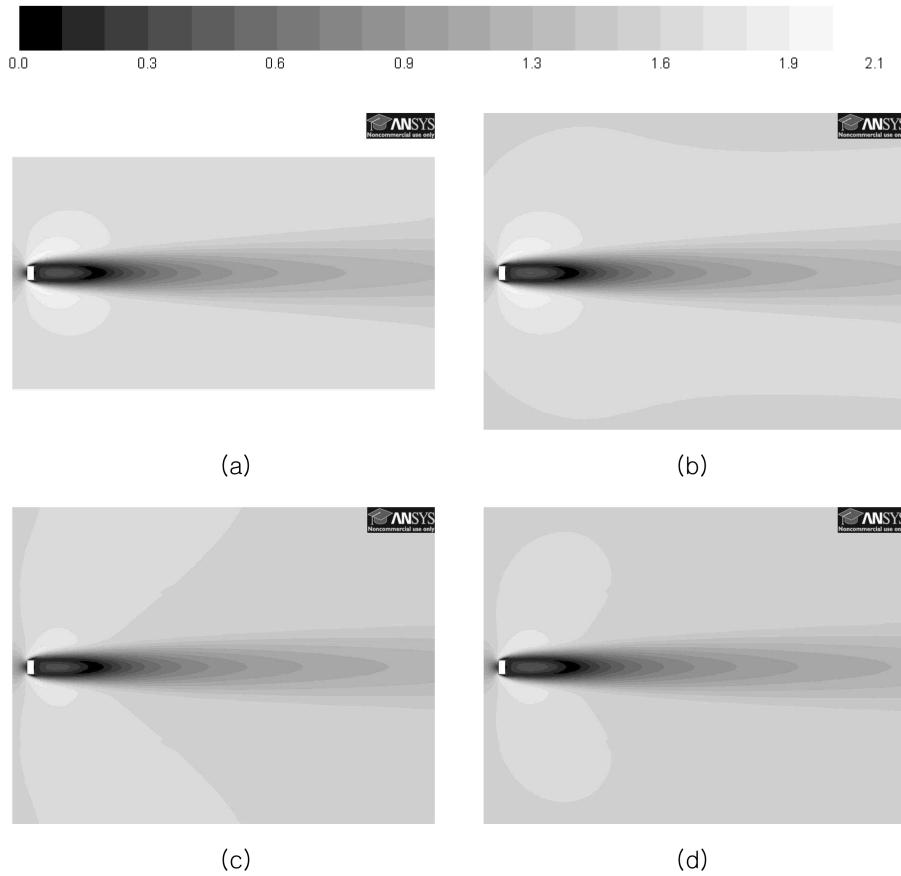


Fig. 4 Contours of velocity magnitude (ms^{-1}) on a horizontal plane at $z=H/2$ for the (a) small, (b) medium 1, (c) medium 2 and (d) large domains

domains. At first glance, they all present a very similar wake pattern, showing, as might be expected with a steady *RANS* simulation, a symmetrical wake. The free stream velocity appears to be higher for the small domain than for the three other domains. This is due to the proximity of the lateral boundaries to the building and is clearly a blockage issue. For the three other domains, the more distant lateral boundaries serve to reduce this effect.

Similarly, Fig. 5 shows contour plots of the velocity magnitude on a vertical plane, located at the centre of the domain. As in Fig. 4, the general pattern is very similar for the four domains. There is a low velocity region located at about $H/2$ downstream and at mid-height of the building for the four domains, which corresponds to the centre of the major recirculation behind the building. Again, for the small domain the flow does not fully recover to the freestream near the top boundary as it does for the two Medium and the Large domains.

The velocity profiles upstream and downstream the building for the Small, Medium 1 and Large domains, are shown in Fig. 6. Also, shown in the figure is the so-called Proposed domain, which will be discussed in Section 4. Upstream of the building, a slight decay in the streamwise velocity can be observed for the large domain, which can be attributed to the much longer fetch upstream the building. The velocity profiles downstream the building in the wake do not highlight any significant differences between the three domains. This tends to indicate that the four domains have

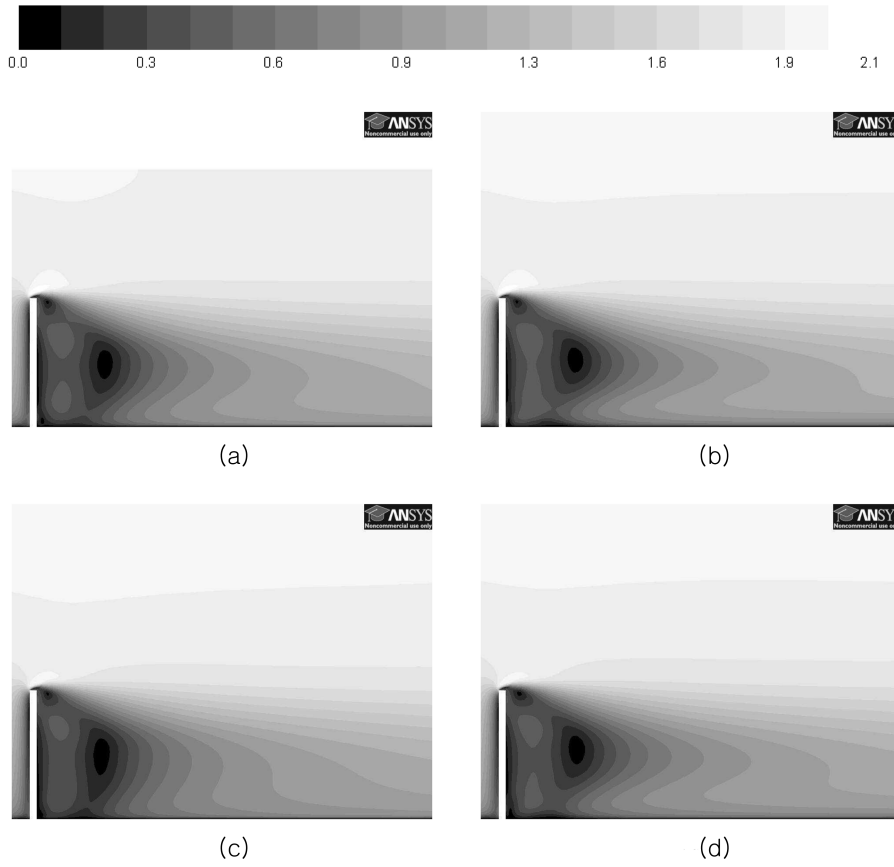


Fig. 5 Contours of velocity magnitude (ms^{-1}) on a vertical plane at $y=0$ for the (a) small, (b) medium 1, (c) medium 2 and (d) large domains

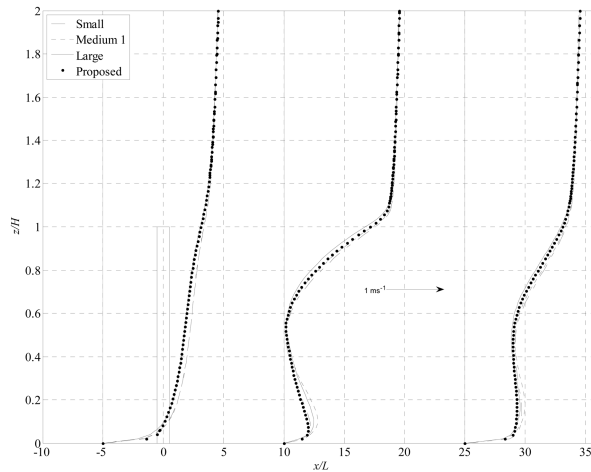


Fig. 6 Comparison of velocity profiles on vertical rakes at $y=0$ and $5L$ upstream, $10L$ downstream and $25L$ downstream of the building for the Small, Medium 1, Large and Proposed domains. The scale is indicated by the annotated arrow

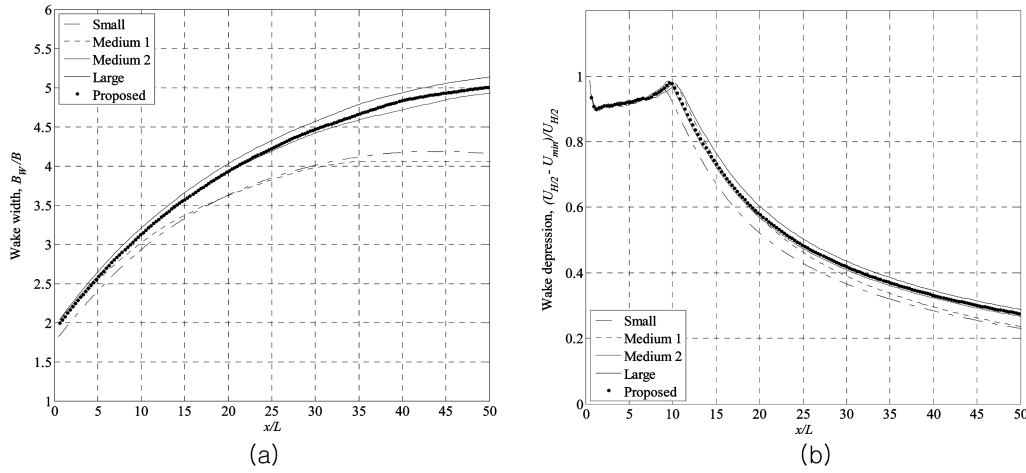


Fig 7 Comparison of (a) wake widths and (b) wake depressions for all domains

their lateral boundaries located far enough from the building so as not to significantly influence the flow in the wake.

In order to investigate this further, a “width of the wake”, B_w , was computed on a horizontal plane at the mid-height of the building for the four domains. It is presented in non-dimensionalised form in Fig. 7(a). The wake was defined to be the region in which the velocity is lower than $0.9 U_{H/2}$, where $U_{H/2}$ is free stream velocity at a height $H/2$ as determined from Eq. (10). Here, the Small and Medium 1 domains have similarly sized wake widths, whereas the Medium 2 and Large domains form another group. It is not clear how the extra upwind fetch of the Medium 2 domain (over the Medium 1 domain) should lead to a much wider wake, when it might be expected that the lateral boundaries would play more of a role. A more convincing argument is that the change in the velocity profile between the two Medium domains is responsible for the difference.

To provide further quantitative data, Fig. 7(b) shows the behaviour of the so-called “wake depression”, which is defined here as the $(U_{H/2} - U_{min})/U_{H/2}$, where U_{min} is the minimum value of velocity on a horizontal line at right angles to the wind direction. So, a value of 1 for the wake depression equates to zero velocity magnitude, as can be seen for all domains at a distance $x \sim 10L = H/2$ downstream of the building, which corresponds well with the centre of the low velocity region seen in Fig. 5. From this point, the velocity magnitude recovers back towards $U_{H/2}$. Far from the building, the trend that the smaller domains have a greater depression is clear. This can be explained by the higher blockage ratios in the smaller domains creating higher wind speeds around the building and a more intense wake, the strength of which is related to the free stream velocity. Evidence for this can be found in Eskridge and Hunt (1979), who look, theoretically, at the development of a wake behind a moving vehicle.

Finally, pressure coefficients along several lines over the building are presented in Figs. 8(a) to (c). The locations of the lines are shown in Fig. 8(d) and on the plots, the non-dimensionalised distance along each line s/L is used, where s is the distance from the start of the line. Notice that some data was not plotted for lines (a) and (b), which extend only $0.8L$ below the top of the building. The pressure coefficient, C_p , is defined as

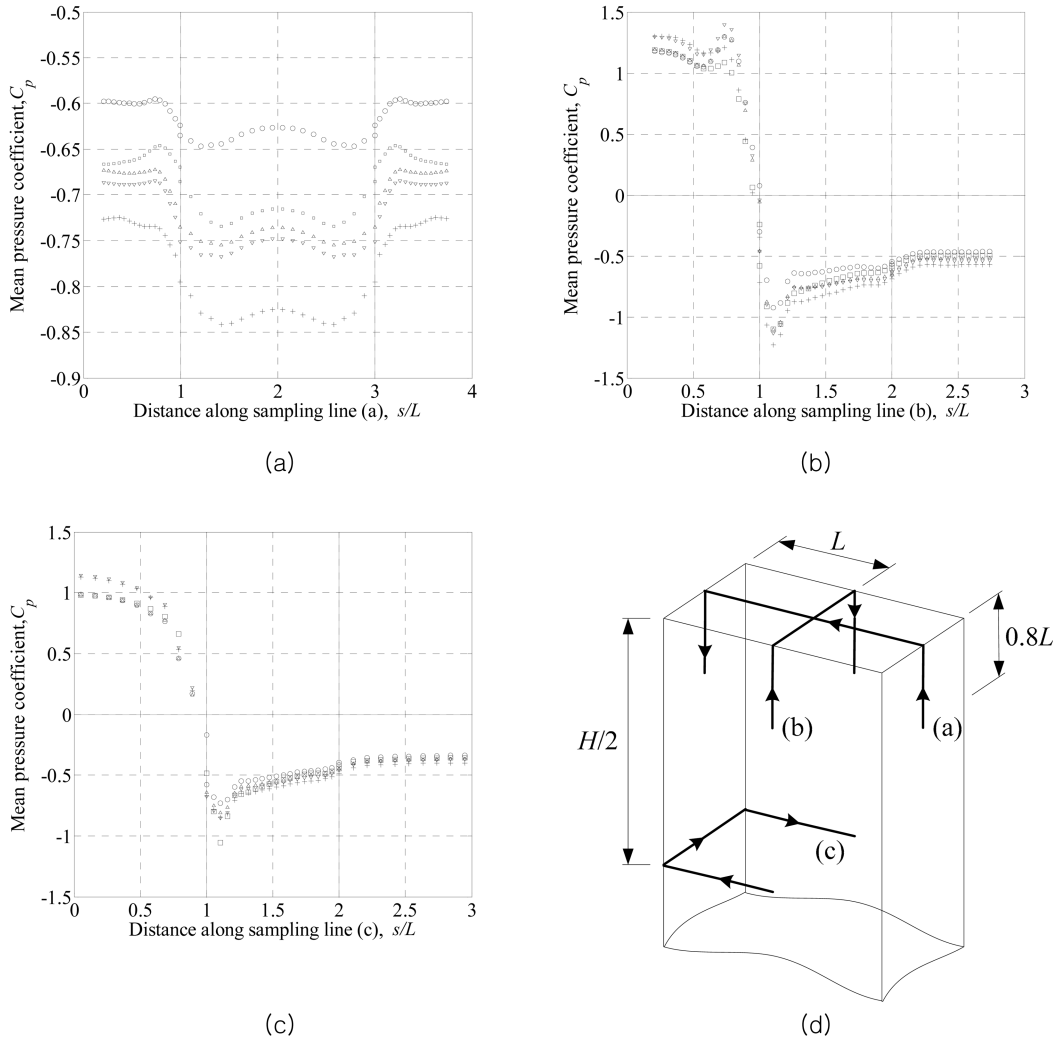


Fig. 8 Pressure coefficients, C_p , on sampling lines (a), (b) and (c), shown in plot (d) for all domains. Legend: + Small; ∇ Medium 1; Δ Medium 2; \circ Large; \square Proposed

$$C_p = \frac{p - p_{\text{ref}}}{\frac{1}{2}\rho U_H^2} \tag{14}$$

where U_H is the wind speed at height H on the inlet plane and p_{ref} is defined as the average pressure on the outlet, in this case 0 Pa relative. It should be noted that the pressure coefficients deliberately are not corrected by the free stream velocity in the domain, as this would be the equivalent of applying a blockage ratio correction to the results. The lines (a) and (b) shown in Fig. 8(d) have been deliberately chosen to pass over the roof because this is where much of the interest for low-rise buildings lies. Pressures on the roof are less of an issue when analyzing the dynamic response of a tall building, which is often driven by pressure differences between the long, vertical walls of the building. Nonetheless, the pressures acting on the roof of a high-rise building are still important

in terms of debris release during storms, for example. The pressure coefficients appear to be more sensitive to the blockage ratio than does the velocity. The pressure coefficients on line (a) display higher suction on the roof for the Small and both Medium domains than for the Large domain. The difference between the two Medium domains is small, the difference being due to the reduction in the velocity in the longer upwind fetch of the Medium2 domain. Indeed, some of the 40% difference between the Small and Large domains can be attributed to the difference in velocity at $z = H/2$ shown in Fig. 6 for the profile at $x = -5L$. Here, the velocity ratio between the Small and Large domains at building height is $7.5/6.5$, which when squared gives a difference of about 30%, in line with the difference seen in the pressure coefficients. However, there must be a blockage effect also, with considerable speedup of the flow above the building in the Small domain when compared with the Large domain. This would indicate that the Franke *et al.* (2004) proposal of the domain height of $6H$, or something close to that, should be followed.

Fig. 8(b) paints a less dramatic picture, but this is due to the much greater range of pressure coefficients seen on this line. At the point at which lines (a) and (b) cross in the centre of the roof, there is still the large discrepancy in C_p between the Small and Large domains. However, on the front face ($0.2 < s/L < 1$), the differences between the domains are less than 20%. The fact that the Medium 2 and Large domains agree more closely on the front face in both plots (b) and (c), indicates that the pressures here are very sensitive to any decay in the velocity profile for these slightly longer upwind fetches. However, the Large domain still has an upwind fetch twice that of the Medium 2 domain, but this would indicate that a shorter upwind fetch, here $20B$, than that suggested by Franke *et al.* (2004) is acceptable.

The pressure coefficients on the leeward face, in Figs. 8(b) and (c) indicate that choosing a much larger downstream distance is not going to greatly influence the results. Therefore, a downstream distance of $30B$ seems to be enough to let the wake develop, without any danger of the outlet boundary unduly influencing the results. The pressure coefficients on the side face at mid-height of the building, $1 < s/L < 2$, indicate that the Medium 2 and Large domains produce results that are within 10% of each other, except in the critical zone just downstream of the leading edge of the building.

Finally, in Table 2 the drag coefficients for the building are presented to provide an additional means of comparing the different simulations. As might be expected from the discussion of pressure coefficients above, the difference in mean drag coefficient, C_d , is greatest between the Small and Large domains. It can also be seen that the Medium 2 domain is closer than the Medium 1 domain. The drag coefficient is given by

$$C_d = \frac{F_x}{\frac{1}{2}\rho U_H^2 BH} \quad (15)$$

where F_x is the force acting in the x -direction.

4. Proposed domain size

It is clear that pressure coefficients and velocity fields are sensitive to domain size, which confirms observations from wind tunnel studies over a period of many years. Assuming the Large domain produces results of the most reliable quality, under the premise that infinitely distant

boundaries would be desirable, the Small domain is simply too small to provide accurate results. This suggests that the 3% blockage ratio suggested by *VDI* is not acceptable. In light of this and the other findings presented in Section 3, the following “Proposed” domain is tentatively suggested

- An upwind fetch, l_u of $20 B$ or $2 H$, whichever is the greater.
- A downwind fetch, l_d , of $30 B$ or $3 H$, whichever is the greater.
- A top clearance, h_s , of $4 H$.
- Side clearances, b_d and b_g of $26 B$.

which can be compared with the corresponding recommendations of Franke *et al.* (2004), which are: $5 H$, $15 H$, $5 H$ and $5 H$ respectively – the comparison is also presented in a slightly different form in Table 2. For the specific case presented here, this represents a reduction in the volume of the domain of approximately 90%. So, in order to test these recommendations, a new domain was created, based on these recommendations.

Fig. 9 shows the flow field of the velocity for the Proposed and Large domains. Qualitatively, similar flow fields are obtained with both domains. The point where the velocity reaches a minimum in the wake is located at approximately $H/2$ downstream the building for both domains. The similarity is confirmed by the velocity profiles plotted upstream and downstream the building, as seen in Fig. 6.

Fig. 7(a) shows how the wake width for the Proposed domain sits amongst the other four domains, in particular the Medium 2 and Large domains. This might be expected because the Proposed domain width sits approximately half way between these two domains. In terms of the wake depression, Fig. 7(b), a similar trend is seen. Crucially, the much shorter downwind fetch of the Proposed domain, does not seem to manifest itself, at least up to a distance of $50 L$ from the building.

Finally, the pressure coefficients are presented in Fig. 8. The largest differences between the

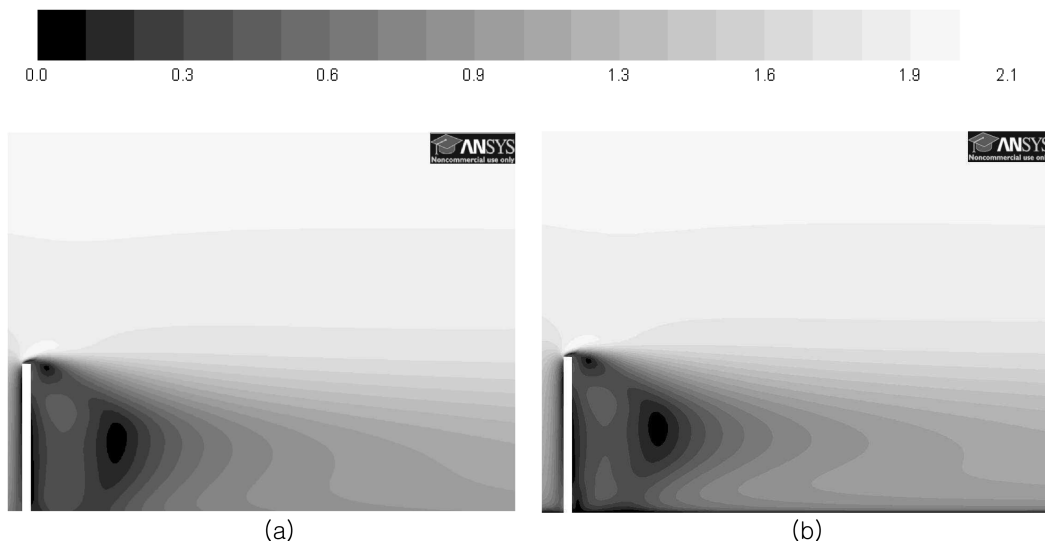


Fig. 9 Contours of velocity magnitude (ms^{-1}) on a vertical plane $y = 0$ for (a) Proposed and (b) large domains

Proposed and Large domains are exhibited on the windward face of the building in plot(a) and amount to a difference of between 15 to 20%. There are concerning differences between the Large and Proposed domains in those regions just downstream of the leading edges of the buildings, plots (b) and (c) with $s/L \approx 1.1$, where the flow separates. In these regions, however, the Proposed domains results in values that are more conservative than the Large domain. As a headline figure, the drag coefficient for the Proposed domain was closer than that of the either of the Medium domains.

5. Conclusions

The aim of this paper is to provide some evidence as to what size of domain to use when modelling tall buildings using *CFD*. As such it extends the admirable work of Franke *et al.* (2004) for low-rise buildings. It should be re-iterated that this was a parametric study with only one parameter, the domain size. The use of a steady *RANS* model in the context of predicting wind loads on buildings has problems (Tamura *et al.* 2008), but the argument used here is that this modelling approach does give an illustrative representation of the blockage effects. A single building was studied in this paper, which means that these findings are by no means universally applicable. For example, as the height of the building is reduced, there will come a point where the recommendations of Franke *et al.* (2004) become applicable again. Perhaps practitioners might interpolate between the findings of this study and those of Franke *et al.* (2004), based on the ratio H/B .

This study was motivated by the fact that the existing guidelines appear to have been defined for low to mid-rise buildings, leading to extremely large computational domains for high aspect ratio structures (height over width), such as slender and tall buildings. Of course, the associated reduction in cell count will depend on the particular application. In the present work, the mesh resolution in the distant parts of the domain was relatively high, especially in the wake region. It could be argued, therefore, that simulations which require a fine mesh in the wake, such as *LES* simulations, might benefit more from the reduced domain size. However, this is with the proviso that the present work used a *RANS* model only. It may be that a shortened downwind fetch might compromise vortex shedding in Detached or Large Eddy Simulations.

With the evidence presented in this paper, researchers might now make more informed decisions about the size of their domains than previously. Indeed, if this paper does nothing more than force workers to test the influence of domain size during their sensitivity studies, it has been a worthwhile process.

References

- Baetke, F. and Werner, H. (1990), "Numerical simulation of turbulent flow over surface mounted obstacles with sharp edges and corners", *J. Wind Eng. Ind. Aerod.*, **35**, 129-147.
- Blocken, B., Roels, S. and Carmeliet, J. (2004), "Modification of pedestrian wind comfort in the Silvertop Tower passages by an automatic control system", *J. Wind Eng. Ind. Aerod.*, **92**(10), 849-873.
- Blocken, B., Stathopoulos, T. and Carmeliet, J. (2007), "CFD simulation of the atmospheric boundary layer: wall function problems", *Atmos. Environ.*, **41**(2), 238-252.
- Braun, A. and Awruch, A. (2009), "Aerodynamic and aeroelastic analyses on the CAARC standard tall building using numerical simulation", *Comput. Struct.*, **87**(9-10), 564-581.
- Buccolieri, R. and Di Sabatino, S. (2007), "Flow and pollutant dispersion in urban arrays for the standardization

- of CFD modelling practise”, *Proceedings of the 11th Conference on Harmonisation within Atmospheric Dispersion Modelling for Regulatory Purposes*, Cambridge, July.
- Eskridge, R. and Hunt, J. (1979), “Highway modeling Part 1: Prediction of velocity and turbulence fields in the wake of vehicles.”, *J. Appl. Meteorol. Clim.*, **18**(4), 387-400.
- Etyemezian, V., Davidson, C.I., Zufall, M., Dai, W., Finger, S. and Striegel, M. (2000), “Impingement of rain drops on a tall building”, *Atmos. Environ.*, **34**(15), 2399-2412.
- Franke, J. (2007), *Introduction to the prediction of wind loads on buildings by computational wind engineering (CWE)*, (Eds. Stathopoulos, T. and Baniotopoulos, C.), *Wind Effects on Buildings and Design of Wind-sensitive Structures*, SpringerWien, New York. chapter 3.
- Franke, J., Hellsten, A., Schlünzen and Carissimo, B. (2007), *Best practice guide for the CFD simulation of flows in the urban environment*, COST Action 732:Quality assurance and improvement of microscale meteorological models.
- Franke, J., Hirsch, C., Jensen, A., Krüs, H., Schatzmann, M., Westbury, P., Miles, S., Wisse, J. and Wright, N.G. (2004), *Recommendations on the use of CFD in wind engineering*, COST Action C14: Impact of Wind and Storm on City Life and Built Environment, von Karman Institute for Fluid Dynamics.
- Hoxey, R., Richards, P. and Short, J. (2002), “A 6 m cube in an atmospheric boundary layer flow Part1. fullscale and wind-tunnel results”, *Wind Struct.*, **5**(2-4), 165-176.
- Huang, S., Li, Q. and Xu, S. (2007), “Numerical evaluation of wind effects on a tall steel structure building by CFD”, *J. Constr. Steel Res.*, **63**, 612-627.
- Ishihara, T. and Hibi, K. (1998), “Turbulent measurements of the flow field around a high-rise building”, *J. Wind Eng. - Japan*, **76**, 55-64.
- Kim, J.J. and Baik, J.J. (2004), “A numerical study of the effects of ambient wind direction on flow and dispersion in urban street canyons using the *RNG k-ε* turbulence model”, *Atmos. Environ.*, **38**(19), 3039-3048.
- Lauder, B. and Spalding, D. (1974), “The numerical computation of turbulent flow”, *Comp. Meth. Appl. Mech. Eng.*, **3**(2), 269-289.
- Mochida, A., Tominaga, Y., Murakami, S., Yoshie, R., Ishihara, T. and Ooka, R. (2002), “Comparison of various *k-ε* models and *DSM* applied to flow around high-rise building - report on *AIJ* cooperative project for *CFD* prediction of wind environment”, *Wind Struct.*, **5**(2), 227-244.
- Revuz, J., Hargreaves, D. and Owen, J. (2010), “Application of a method for generating turbulent inflow based on inverse fourier transforms for large eddy simulations”, *Proceedings of the 5th International Symposium on Computational Wind Engineering*, Chapel Hill, North Carolina, USA, May 23-27.
- Revuz, J. (2011), *Numerical simulation of the wind flow around a tall building and its dynamic response to wind excitation*, PhD Thesis, The University of Nottingham, Nottingham, UK.
- Richards, P. and Hoxey, R. (1993), “Appropriate boundary conditions for computational wind engineering models using the *k-ε* turbulence model”, *J. Wind Eng. Ind. Aerod.*, **46-47**, 145-153.
- Sankaran, R. and Paterson, D. (1997), “Computation of rain falling on a tall rectangular building”, *J. Wind Eng. Ind. Aerod.*, **72**, 127-136.
- So, E., Chan, A. and Wong, A. (2005), “Large-eddy simulations of wind flow and pollutant dispersion in a street canyon”, *Atmos. Environ.*, **39**(20), 3573-3582.
- Spalart, P. (2001), *Young-Person's Guide to Detached-Eddy Simulation Grids*, Technical Report NASA/CR-2001-211032. NASA. Langley Research Centre, Hampton, Virginia, USA.
- Tamura, T., Nozawa, K. and Kondo, K. (2008), “*AIJ* guide for numerical prediction of wind loads on buildings”, *J. Wind Eng. Ind. Aerod.*, **96**(9-10), 1974-1984.
- Tominaga, Y., Mochida, A., Yoshie, R., Kataoke, H., Nozu, T., Yoshikawa, M. and Shirasawa, T. (2008), “*AIJ* guidelines for practical applications of *CFD* to pedestrian wind environment around buildings”, *J. Wind Eng. Ind. Aerod.*, **96**(10-11), 1749-1761.
- VDI (2000), *Environmental meteorology - Physical modelling of flow and dispersion processes in the atmospheric boundary layer - Application of wind tunnels*, Technical Report 3783, Part 12. Verien Deutscher Ingenieure.
- Watakabe, M., Ohashi, M., Okada, H., Okuda, Y., Okuda, Y., Kikitsu, H., Ito, S., Sasaki, Y., Yasui, K., Yoshikawa, K. and Tonagi, M. (2002), “Comparison of wind pressure measurements on tower-like structure obtained from full-scale observation, wind tunnel test, and the *CFD* technology”, *J. Wind Eng. Ind. Aerod.*,

- 90**, 1817-1829.
- Xiang, W. and Wang, H. (2008), "Discussion on grid size and computational domain in *CFD* modelling of pedestrian wind environment around buildings", *J. Civ. Eng. Arch.*, **2**, 8-14.
- Yakhot, V., Orszag, S., Thangam, S., Gatski, T. and Speziale, C. (1992), "Development of turbulence models for shear flows by a double expansion technique", *Phys. Fluids*, **4**(7), 1510-1520.

JH